# Easy access to strongly fluorescent higher homologues of BODIPY†

Lukas Erlemeier, [a] Marius J. Müller, [b] Gina Stuhrmann, [c] Tobias Dunaj, [a] Gunnar Werncke, *[a] Sangam Chatterjee [b] and Carsten von Hänisch *[a]

**We present the easy and high yield synthesis of several group 13 $^{Mes}$DPM compounds (Al–In) with alkyl substituents at the metal atom. All these compounds were fully characterized using techniques including X-ray diffraction analysis and photoluminescence measurements. It shows that for aluminium and gallium pronounced green fluorescence is observed, which is absent for indium. DFT calculations confirm that the first electronic transition corresponds to a ligand-based π–π* transition.**

## Introduction

With the first report of the dipyrromethene (DPM) ligand in 1924 by Fischer and Schubert, the interest in complexes containing such one or more DPM ligands has increased considerably.[1] The initial interest was due to its use in porphyrin synthesis[2] but later it gained further attention owed to the corresponding boron difluoride complexes, called BODIPY(s) (boron difluoride dipyrromethene(s)), and their strongly fluorescent properties.[3–5] The fluorescence of dipyrromethene based compounds is due to a ligand based π*–π emission where the strength of this electronic transition is influenced by the bulkiness of the aryl group at the *meso*-position,[6–9] the dimensions of the conjugated π-system, and the rigidification by chelating cationic species.[10–12] Although the first representatives of BODIPYs were described as early as 1968 by Treibs and Kreuzer, the synthesis of the "parent" BODIPY was not reported until 2009 (Fig. 1a).[13–16] The fascinating optical properties of these compounds, such as sharp fluorescence and high fluorescence quantum yields ($\varphi_F$) of up to 100% in solution,[7,17] led to many different applications, for example as light-harvesting arrays, fluorescent switches or fluorescence labels in the field of biomedical imaging (with low energetic excitation wavelengths).[17–25] In recent years, considerable attention has been paid to research on highly efficient BODIPY containing photosensitizers, which show potential for use in photodynamic therapy.[3,26]

In contrast to the prevalence of BODIPYs, the use of dipyrromethenes as ligands for other main group elements except boron remains scarce. Chisholm *et al.* employed magnesium containing $^{Mes}$DPM (1,5,9-trimesityldipyrromethene) complexes for lactide polymerisation[27] while lactone polymerisation was examined by the Mason group for aluminium containing DPM compounds.[31,32] The ability of bulky DPM ligands to stabilize low-valent metal ions, as exploited for 3d-transition metal complexes,[10,33–37] was shown by Nagendran *via* the divalent germanium compound ($^{Mes}$DPM)GeCl (Fig. 1b).[28] It was put forth recently by Liu *et al.* for low-valent Sb (Fig. 1c) which can cleave disulfides and diselenides.[29] In a few instances, substitution of second row elements (as in BODIPYs) with heavier main group elements can have dramatic impact on a molecule's optical and electronic properties as has been shown for trivalent pnictogenide,[29] low valent germanium (Fig. 1b) and tin[28,38] as well as gallium halides (Fig. 1d)[30,39–43] The redox behaviour and radical stabilization have also been studied recently for DPM based main group compounds.[44–46] Finally, a bismuth compound with this ligand class was also presented only recently.[47]

[a]*Department of Chemistry, Philipps University Marburg, 35032 Marburg, Germany. E-mail: haenisch@chemie.uni-marburg.de, gunnar.werncke@chemie.uni-marburg.de*

[b]*Institute of Experimental Physics I, Justus Liebig University Giessen, 35392 Giessen, Germany. E-mail: sangam.chatterjee@physik.uni-giessen.de*

[c]*Institute of Nanotechnology (INT), Karlsruhe Institute of Technology (KIT), Germany*

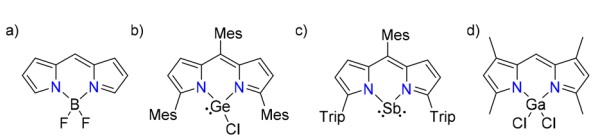


**Fig. 1** Lewis structure of "parent" BODIPY (a), selected literature-known main group DPM complexes of divalent germanium (b) and low valent antimony (c) as well as a DPM gallium halide complex (d).[13,28–30]

In this context, we herein present the facile and high yield synthesis of $^{Mes}$DPM supported triel dialkyl complexes of aluminium to indium as the higher homologues of the well-studied BODIPY. Their solid and solution state photoluminescence properties were investigated.

## Results and discussion

The free (protonated) ligand ($^{Mes}$DPM)H (**1**) was obtained according to literature procedures,[34,48,49] and the missing solid state structure was determined by X-ray diffraction analysis (see the ESI†). **1** was reacted with the trialkyls $MR_3$ (M = Al–In; R = Me, Et) (Scheme 1) in toluene under alkane elimination. It generated the $^{Mes}$DPM triel dialkyls (**2a/b–4a/b**) as red/orange solids in quantitative yields. This makes this procedure an easy and efficient synthesis route, and avoids the intrinsic purification problems encountered during salt elimination reactions.[30,47] It is worth noting that **4a/b** represent the first DPM based compounds of indium. Crystals for all compounds were obtained from saturated toluene solutions at −32 °C and the solid-state structures were determined by X-ray diffraction analysis. The methyl compounds **2a–4a** crystallize isotypically in the monoclinic crystal system with the space group $P2_1/m$ (Fig. 2 left). Here, the mirror plane is aligned with the mesityl ring in the ligand backbone and the central metal. Within the solid-state molecular structures, the metal atoms are coordinated in a distorted tetrahedral fashion ($\tau_4$ and $\tau_4' \geq 0.84$), where the distortion increases with the atomic order from aluminium to indium. Comparing **2a** with a similar aluminium compound ($^{Ph}$DPM)$AlMe_2$ from the Mason group, using *meso*-phenyl-α,α′-dimesityldipyrromethene as a ligand, the bond lengths displayed in Table 1 show no significant deviations, with only the N–M–N bond angle of **2a** being slightly larger (94.25(5)°) compared to the literature (($^{Ph}$DPM)$AlMe_2$: 92.2 (1)°).[31] Within the complexes, the metal atom is symmetrically coordinated by the $^{Mes}$DPM ligand, which is also reflected by its proton NMR spectroscopic signature in solution. The $^1$H NMR spectra further show an increasing downfield shift for the metal bound methyl groups from aluminium (−0.72 ppm) to indium (−0.29 ppm) in line with expectations.[50] In contrast to the methyl compounds, **2b** and **3b** crystallize in the triclinic crystal system with the space group $P2_1/m$ while **4b** crystallizes in the monoclinic crystal system with the space group $P2_1/c$ (Fig. 2 right). Their molecular structures do not contain a crystallographic symmetry element. As for **2a–4a**, the diethyl compounds **2b–4b** show increasing bond lengths around the metal centre going from aluminum to indium, while the N–M–N bond angles decrease. Compared to **2a–4a**, the change to diethyl substitution in **2b–4b** has no significant impact on the structural metrics of the metal centre. During the synthesis it became evident that particularly the methyl compounds **2a** and **3a** exhibit an intense green fluorescence in solution upon solar irradiation (Fig. 3). This prompted UV/Vis spectroscopic and photoluminescence measurements in solution and in the solid state.

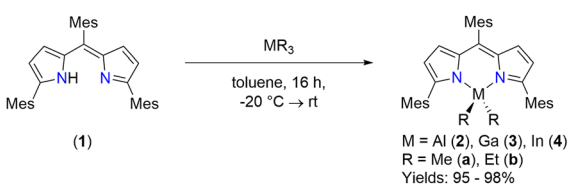


**Scheme 1** Synthesis of the desired group 13 $^{Mes}$DPM complexes **2a/b–4a/b**.

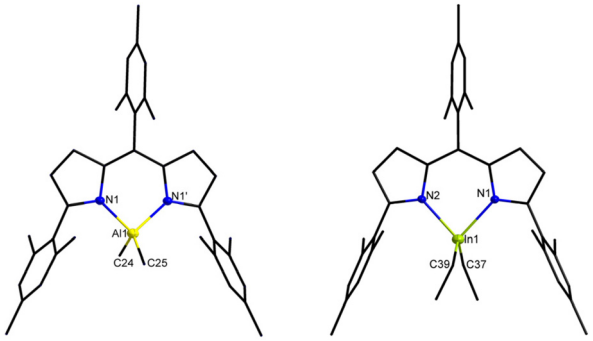


**Fig. 2** Exemplary solid-state molecular structures of ($^{Mes}$DPM)$AlMe_2$ (**2a**, left) and ($^{Mes}$DPM)$InEt_2$ (**4b**, right) with thermal ellipsoids set at the 50% probability level (colour scheme: C = black; N = blue; and Al = yellow). C atoms are depicted as balls and sticks and H atoms are omitted for clarity.

**Table 1** Selected bond lengths and angles of **2–4a/b**

| Compound | $d_{M\ N}$/Å | $d_{M\ C}$/Å | $\sphericalangle_{N\ M\ N}$/° | $\tau_4$ | $\tau_4'$ |
|---|---|---|---|---|---|
| **2a** | 1.9399(9) | 1.963(2) | 94.25(5) | 0.94 | 0.93 |
| | 1.9400(9) | 1.964(2) | | | |
| **3a** | 1.9983(8) | 1.969(2) | 92.34(5) | 0.91 | 0.89 |
| | 1.9984(8) | 1.967(2) | | | |
| **4a** | 2.196(3) | 2.147(6) | 85.1(2) | 0.87 | 0.84 |
| **2b** | 1.928(3) | 1.956(4) | 94.4(1) | 0.92 | 0.91 |
| | 1.932(3) | 1.962(4) | | | |
| **3b** | 1.993(2) | 1.962(2) | 92.07(7) | 0.89 | 0.89 |
| | 1.993(2) | 1.974(2) | | | |
| **4b** | 2.196(2) | 2.158(3) | 85.35(9) | 0.87 | 0.84 |
| | 2.195(2) | 2.150(3) | | | |

$d_{A\ B}$ = bond length of the AB bond and $\sphericalangle_{A\ B\ C}$ = bond angle.

The solid-state UV/Vis measurements (Fig. 4) reveal several absorptions in the ultraviolet region (200–380 nm) and a maximum absorption $\lambda_{max,ss}$ in the range between 502 nm and 513 nm, comparable to other examples of this class of compounds and fitting to the green part of the visible spectrum (Table 2).[17,28,29,31,32] Here, it is prominent that the aluminium and indium compounds (**2a/b** & **4a/b**) show nearly identical $\lambda_{max}$ values while the signals for the gallium compounds (**3a/b**) are slightly blue shifted. Similar results were obtained from UV/Vis spectra in toluene solution with an absorption maxima $\lambda_{max}$ of around 500 nm (for spectra see the ESI†) giving molar absorption coefficients at the maximum absorption in the range $1.1 \times 10^5$ to $1.5 \times 10^5$ L mol$^{-1}$ cm$^{-1}$ (Table 2). Next, we

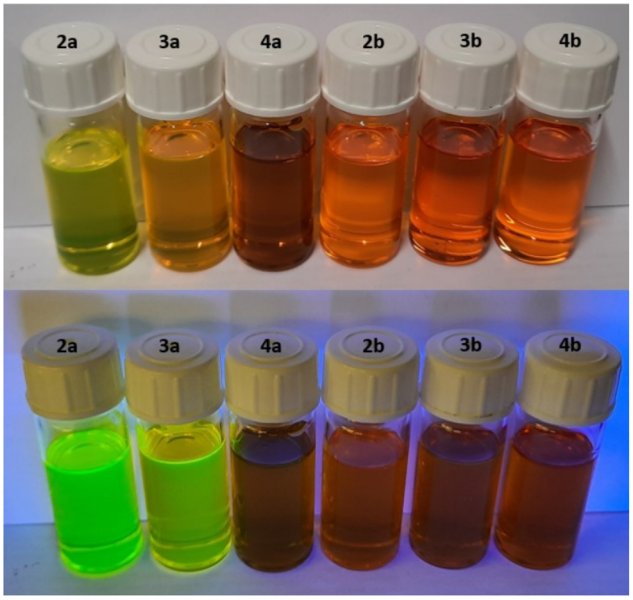


**Fig. 3** Samples of $^{Mes}$DPM triel dialkyls (**2a/b–4a/b**) in toluene with no irradiation (top) and irradiation with 366 nm (bottom). Samples from left to right: **2a**, **3a**, **4a**, **2b**, **3b** and **4b**.

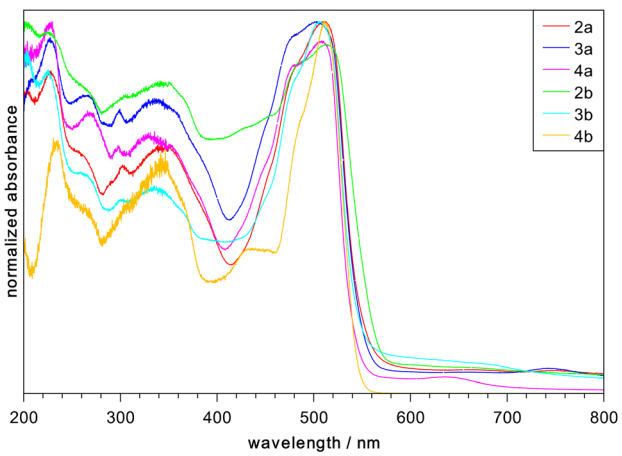


**Fig. 4** Normalized and stacked solid-state UV/Vis spectra of the synthesized $^{Mes}$DPM triel complexes ($^{Mes}$DPM)$MMe_2$ **2a–4a** and ($^{Mes}$DPM)$MEt_2$ **2b–4b** (colour scheme: red = **2a**; blue = **3a**; violet = **4a**; green = **2b**; turquoise = **3b**; and yellow = **4b**).

carried out excitation and emission spectroscopic measurements in toluene solution (see the ESI†). The measurements for **2a–4a** and **3b** show a strong absorption ($\lambda_{Ex}$) around 340 nm and fluorescence signals ($\lambda_{Em}$) in the range of 517 to 536 nm (see ESI†), while for **2b** and **4b** no fluorescence was detected. For the solid-state photoluminescence spectroscopic measurements, samples of the corresponding compounds were irradiated using a 325 nm He–Cd continuous wave laser. The resulting spectra (Fig. 5) reveal a quite sharp fluorescence emission ($\lambda_F$) around 560 nm which matches with green light and the already visually perceived observations. The corresponding measurements in toluene solution using a 405 nm continuous wave diode laser were also carried out (Fig. 6). The fluorescence emission maximum in solution is found at 540 nm which consistently differs from the one in the solid state by ≈20 nm. We were further able to determine the fluorescence quantum efficiencies $\varphi_F$ using the obtained photoluminescence spectra. In the solid state the measurements gave quantum yields $\varphi_{F,ss}$ for the two dimethyl compounds **2a** and **3a** of about 34%. The corresponding examination in toluene solution gave slightly higher quantum yields of 44% for **2a** and 51% for **3a**. The solution state photoluminescence behaviour, especially of **2a** and **3a**, is comparable to that of a few other heavier triel DPM compounds, which can reach up to 90%. In contrast, reports on the solid-state fluorescence quantum yields of related heavier BODIPYs are so far lacking.[30,51] Therefore, the solid-state values obtained for **2a** and **3a** are the best compared to those of highly fluorescent BODIPYs, whose solid-state quantum yields range from 0 to about 30%.[52,53] This strong discrepancy between fluorescence

**Table 2** Photoluminescence data for $LMX_2$ (**2–4a/b**)

| | $\lambda_{max,ss}$/ nm | $\lambda_{max}$/ nm | $\varepsilon_{max}$ ($\lambda_{max}$)/L mol$^{-1}$ cm$^{-1}$ | $\lambda_F$/ nm | $\varphi_F$/ % | $\lambda_{F,ss}$/ nm | $\varphi_{F,ss}$/ % |
|---|---|---|---|---|---|---|---|
| **2a** | 509 | 504 | $1.27 \times 10^5$ | 540 | 44 | 562 | 34 |
| **3a** | 502 | 500 | $1.30 \times 10^5$ | 539 | 51 | 562 | 33 |
| **4a** | 509 | 499 | $1.43 \times 10^5$ | 540 | 2 | 557 | 3 |
| **2b** | 513 | 505 | $1.30 \times 10^5$ | 551 | <1 | 564 | <1 |
| **3b** | 505 | 502 | $1.10 \times 10^5$ | 545 | 2 | 563 | <1 |
| **4b** | 512 | 505 | $1.49 \times 10^5$ | 547 | <1 | 567 | <1 |

L = $^{Mes}$DPM, $\lambda_{max,ss}$ = absorption maximum (solid-state), $\lambda_{max}$ = absorption maximum (toluene solution), $\varepsilon_{max}$ ($\lambda_{max}$) = molar absorption coefficient (at $\lambda_{max}$), $\lambda_F$ = fluorescence maximum (toluene solution), $\varphi_F$ = fluorescence quantum yield (toluene solution), $\lambda_{F,ss}$ = fluorescence maximum (solid-state), and $\varphi_{F,ss}$ = fluorescence quantum yield (solid-state).

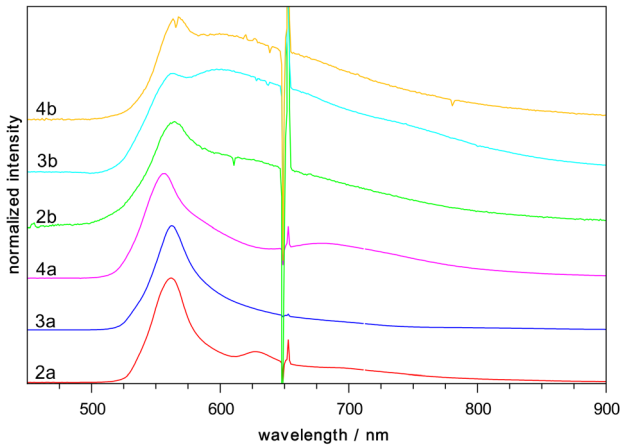


**Fig. 5** Normalized and stacked solid-state photoluminescence spectra of the synthesized $^{Mes}$DPM triel complexes (colour scheme: red = **2a**; blue = **3a**; violet = **4a**; green = **2b**; turquoise = **3b**; and yellow = **4b**). Excitation with a 325 nm He–Cd continuous wave laser (the signal at 650 nm is the second diffraction order of the laser).

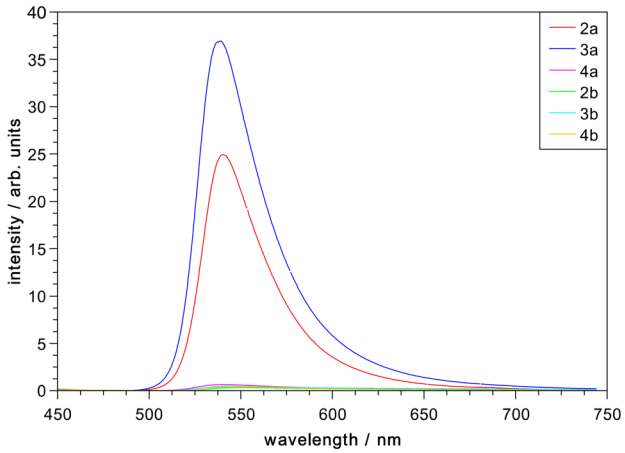


Fig. 6 Photoluminescence spectra of the synthesized $^{Mes}$DPM triel complexes in toluene (colour scheme: red = **2a**; blue = **3a**; violet = **4a**; green = **2b**; turquoise = **3b**; and yellow = **4b**). Excitation with a 405 nm diode laser.

quantum efficiencies in solution and in the solid state is well-known in the literature and is due to strong intermolecular interactions in the solid-state leading to fluorescence quenching.[52,53] However, for the indium compound **4a**, the fluorescence quantum efficiency drops down to 3%, and respectively to 2% in the solid state. This can be attributed to the heavy atom effect, known to enhance other (non-emissive) radiative pathways such as inter-system-crossing,[30,47,54,55] or lesser rigidity of the π-system due to the considerably larger In–N bonds (Table 1). For the corresponding diethyl compounds **2b**–**4b** very low quantum efficiencies below 2% were obtained, irrespective of whether they were measured in the solid state or in solution. The overall reduced fluorescence of the ethyl derivatives with regard to their methyl congeners can be attributed to the larger number of vibrational degrees of freedom of the ethyl substituted compounds. All compounds exhibit very similar fluorescence maxima and stoke shifts. This shows a HOMO–LUMO gap that is unaffected by the identity of the central metal and its substituents, which aligns with observations made for other heavier main-group BODIPY analogues. Indeed, the computed first electronic transition of the different dipyrromethene dimethyl triel complexes (**2a**, **3a** and **4a**) on a CPCM-CIS(D)/def2-TZVPP//r$^2$scan-3c level gave virtually identical excitation, which belongs to a ligand centered $\pi \rightarrow \pi^*$ transition (Fig. 7). This is in agreement with observations made for a dichloro gallium dipyrromethene compound (Fig. 1d) and a very recent report on related group 15 dihalides.[30,47]

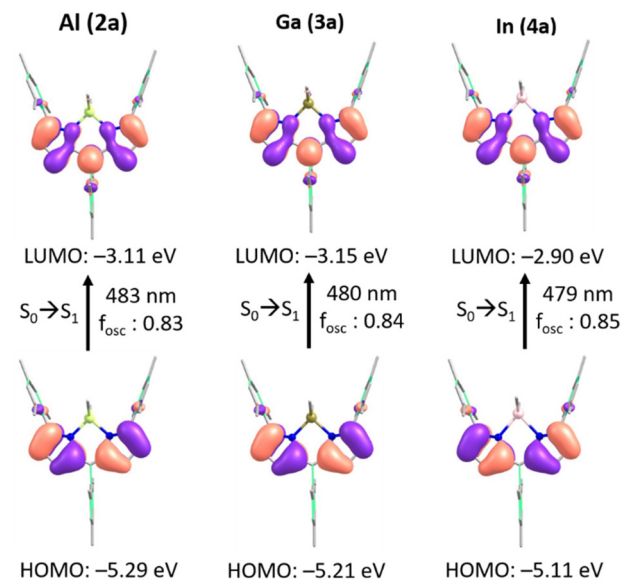


Fig. 7 Computed first electronic excitation of the dipyrromethene dimethyl triel compounds **2a**, **3a** and **4a** (CPCM-CIS(D)/TZVPP) and absolute HOMO/LUMO energies (r$^2$SCAN-3c).

## Conclusions

In conclusion, the facile and high-yielding synthesis of group 13 dipyrromethene complexes (Al–In) with two alkyl substituents (Me and Et) at the metal centre is described. These compounds were examined for their photoluminescence behaviour in solution and in the solid state, the latter being unreported for heavier main-group dipyrromethenes. This gave fluorescence quantum yields in the solid state of up to $\varphi_F$ = 34% for aluminium and gallium. Introducing indium as the central atom or larger alkyl substituents leads to substantial fluorescence quenching. Considering these results, elucidation of volatile aluminium and gallium compounds for the deposition of optically active layers will be pursued in the future.

## Experimental

### General synthetic considerations

All manipulations were performed under an inert argon atmosphere using standard Schlenk techniques. The handling and storage of moisture or air sensitive substances occurred under an inert argon atmosphere in a glove box. Solvents were dried by standard procedures and freshly distilled before use. Sodium pyrrolide,[56] mesitaldehyde dimethyl acetal,[57] 2-Mes-1*H*-pyrrole,[48] pyridinium *p*-toluenesulfonate (PPTS),[58] and 1,5,9-trimesityldipyrromethene ($^{Mes}$DPM)[34] were prepared according to literature methods. All trialkyl group 13 compounds ($MR_3$; M = Al–In, R = Me, Et) were received from Dockweiler Chemicals and used without further purification.

At room temperature, 0.15 g DPM$^{Mes}$H (**1**, 0.30 mmol, 1.00 eq.) was suspended in 10 mL toluene under stirring. To this suspension $MR_3$ (M = Al–In; R = Me, Et) (0.30 mmol, 1.00 eq.) was added dropwise. The reaction mixture was stirred at room temperature for 16 h. Evaporation of the solvent and drying under reduced pressure at 85 °C afforded the desired products ((DPM$^{Mes}$)$MR_2$ (M = Al–In; R = Me, Et)) as red/orange solids in almost quantitative yields between 95 and 98%.

### Analytical methods

For NMR spectroscopic experiments a Bruker AV II 300 MHz, AV III HD 250 MHz or a AV III 500 MHz was used. Coupling constants ($J$) were reported in Hertz (Hz) and the chemical shifts ($\delta$) were given in ppm relative to the standard ($^1$H, $^{13}$C: $SiMe_4$). The NMR multiplicities are abbreviated with s = singlet, d = doublet, t = triplet, q = quartet or m = multiplet. The assignment of $^{13}$C and $^1$H signals was made using 2D NMR spectroscopy.

IR spectra were recorded on a Bruker ALPHA FT-IR with a diamond ATR (500–4000 cm $^{1}$). Elemental analyses were performed on an ELEMENTAR Vario Microcube and the content is reported in %.

HR-CI mass spectra were acquired with an AccuTOF GCv 4G (JEOL) Time of Flight (TOF) mass spectrometer. An internal or external standard was used for drift time correction.

Single crystal X-ray diffraction experiments were performed at 100 K on a D8-Quest diffractometer by Bruker with MoKα radiation ($\lambda$ = 0.71073) or with a StadiVari diffractometer by STOE with CuKα radiation ($\lambda$ = 1.54186).

Solid-state UV/Vis spectroscopic measurements were performed in reflection under inert conditions employing a Varian Cary 5000 UV/Vis/NIR spectrometer from Agilent, equipped with a Praying Mantis accessory. Extinction spectra were recorded from 2 μM toluene solutions under an inert atmosphere at 298.15 K on an Analytik Jena Specord S600 using WinASPECT software and an UNISOKU CoolSpeK Cryostat. Excitation and emission spectra were measured in solution on a Varian Cary Eclipse fluorescence spectrometer from Agilent with a xenon flash lamp. Photoluminescence spectroscopy in the solid state and quantum yield measurements are performed on powdered compounds. They are transferred into a 1 mm inner diameter quartz-glass cuvette under inert conditions. The sample is then mounted in an integrating sphere and is directly excited by a 325 nm He–Cd continuous wave laser. The emission is spectrally resolved in a 50 cm Czerny–Turner spectrograph and detected by a thermoelectrically cooled Si CCD camera using appropriate order-suppressing color filters. Corrections for the setup response and the integrating sphere emission are performed according to the literature.[59] The maximum wavelength ($\lambda_i$) of the received signals from spectroscopic measurements (UV/Vis and PL) are given in nm and calculated fluorescence quantum efficiencies ($\varphi_F$) are reported in %.

For photoluminescence spectroscopy in solution (2 mg L $^{1}$ in toluene), a similar setup featuring a 405 nm continuous wave diode laser is used. The quantum efficiencies are validated against a solution of perylene in ethanol.[60]

### Computational analysis

The calculations were performed with ORCA v. 5.0.4.[61–64] The geometries of **2a**, **3a** and **4a** were optimised on the r$^2$scan-c3 level of theory[65] starting from the solid state structures obtained from the X-ray diffraction analysis. All optimized structures were verified as true minima by the absence ($N^{imag}$ = 0) of negative eigenvalues in the harmonic vibrational frequency analysis. The first electronic transition of these structures was refined at the CIS(D)/def2-TZVPP level using toluene in the implicit CPCM solvent method.[66–68]

## Conflicts of interest

There are no conflicts to declare.

## Author contributions

Lukas Erlemeier: synthesis, characterization, sample preparation, implementation of single crystal XRD and crystal structure refinement, and writing of the manuscript. Marius J. Müller: measurement of photoluminescence spectra in solution and in the solid state as well as determination of quantum efficiencies. Gina Stuhrmann: measurement of excitation and emission spectra and implementation of UV/Vis spectroscopy in the solid state and single crystal XRD. Tobias Dunaj: crystal structure refinement and implementation of single crystal XRD. Gunnar Werncke: scientific management of the project and writing of the manuscript. Sangam Chatterjee: scientific management of optical measurements and writing of the manuscript. Carsten von Hänisch: scientific management of the project and writing of the manuscript.

## Acknowledgements

C. G. W. and C. V. H. acknowledge the Deutsche Forschungsgemeinschaft (DFG) for funding (WE 5627/4-2 and HA 3466/11-1). We thank Dr. Sergei Ivlev (Philipps-Universität Marburg) for his important help with the crystal structures.

## References

1 H. Fischer and M. Schubert, *Ber. Dtsch. Chem. Ges. B*, 1924, **57**, 610–617.
2 R. Tschesche, *Angew. Chem., Int. Ed.*, 1938, **51**, 27–27.
3 G. Linden and O. Vázquez, *Chem. – Eur. J.*, 2020, **26**, 10014–10023.
4 D. Van Vranken and G. A. Weiss, *Introduction to Bioorganic Chemistry and Chemical Biology*, Garland Science, New York, London, 2018.
5 J. O. Escobedo, O. Rusin, S. Lim and R. M. Strongin, *Curr. Opin. Chem. Biol.*, 2010, **14**, 64–70.
6 I. V. Sazanovich, C. Kirmaier, E. Hindin, L. Yu, D. F. Bocian, J. S. Lindsey and D. Holten, *J. Am. Chem. Soc.*, 2004, **126**, 2664–2665.
7 T. Rohand, W. Qin, N. Boens and W. Dehaen, *Eur. J. Org. Chem.*, 2006, **2006**, 4658–4663.
8 R. Sakamoto, T. Iwashima, M. Tsuchiya, R. Toyoda, R. Matsuoka, J. F. Kögel, S. Kusaka, K. Hoshiko, T. Yagi,

T. Nagayama, *et al.*, *J. Mater. Chem. A*, 2015, **3**, 15357–15371.
9 N. Sakamoto, C. Ikeda, M. Yamamura and T. Nabeshima, *J. Am. Chem. Soc.*, 2011, **133**, 4726–4729.
10 A. B. Scharf, S. L. Zheng and T. A. Betley, *Dalton Trans.*, 2021, **50**, 6418–6422.
11 M. A. Filatov, A. Y. Lebedev, S. N. Mukhin, S. A. Vinogradov and A. V. Cheprakov, *J. Am. Chem. Soc.*, 2010, **132**, 9552–9554.
12 C. Ikeda, S. Ueda and T. Nabeshima, *Chem. Commun.*, 2009, 2544–2546.
13 A. Treibs and F.-H. Kreuzer, *Liebigs Ann.*, 1968, **718**, 208–223.
14 I. J. Arroyo, R. Hu, G. Merino, B. Z. Tang and E. Peña-Cabrera, *J. Org. Chem.*, 2009, **74**, 5719–5722.
15 K. Tram, H. Yan, H. A. Jenkins, S. Vassiliev and D. Bruce, *Dyes Pigm.*, 2009, **82**, 392–395.
16 A. Schmitt, B. Hinkeldey, M. Wild and G. Jung, *J. Fluoresc.*, 2009, **19**, 755–758.
17 A. Loudet and K. Burgess, *Chem. Rev.*, 2007, **107**, 4891–4932.
18 R. Ziessel, G. Ulrich and A. Harriman, *New J. Chem.*, 2007, **31**, 496–501.
19 G. Ulrich, R. Ziessel and A. Harriman, *Angew. Chem., Int. Ed.*, 2008, **47**, 1184–1201.
20 R. Ziessel, G. Ulrich, A. Haefele and A. Harriman, *J. Am. Chem. Soc.*, 2013, **135**, 11330–11344.
21 C. Trieflinger, K. Rurack and J. Daub, *Angew. Chem., Int. Ed.*, 2005, **44**, 2288–2291.
22 T. A. Golovkova, D. V. Kozlov and D. C. Neckers, *J. Org. Chem.*, 2005, **70**, 5545–5549.
23 A. C. Benniston and G. Copley, *Phys. Chem. Chem. Phys.*, 2009, **11**, 4124–4131.
24 M. Yee, S. C. Fas, M. M. Stohlmeyer, T. J. Wandless and K. A. Cimprich, *J. Biol. Chem.*, 2005, **280**, 29053–29059.
25 R. W. Wagner and J. S. Lindsey, *Pure Appl. Chem.*, 1996, **68**, 1373–1380.
26 E. Garanger, E. Aikawa, F. Reynolds, R. Weissleder and L. Josephson, *Chem. Commun.*, 2008, 4792–4794.
27 M. H. Chisholm, K. Choojun, J. C. Gallucci and P. M. Wambua, *Chem. Sci. J.*, 2012, **3**, 3445–3457.
28 C. K. Jha, S. Karwasara and S. Nagendran, *Chem. – Eur. J.*, 2014, **20**, 10240–10244.
29 C. Liu, Y. Dai, Q. Han, C. Liu and Y. Su, *Chem. Commun.*, 2023, **59**, 2161–2164.
30 W. Wan, M. S. Silva, C. D. McMillen, S. E. Creager and R. C. Smith, *J. Am. Chem. Soc.*, 2019, **141**, 8703–8707.
31 C. G. Gianopoulos, K. Kirschbaum and M. R. Mason, *Organometallics*, 2014, **33**, 4503–4511.
32 C. G. Gianopoulos, N. Kumar, Y. Zhao, L. Jia, K. Kirschbaum and M. R. Mason, *Dalton Trans.*, 2016, **45**, 13787–13797.
33 E. R. King, G. T. Sazama and T. A. Betley, *J. Am. Chem. Soc.*, 2012, **134**, 17858–17861.
34 E. R. King and T. A. Betley, *Inorg. Chem.*, 2009, **48**, 2361–2363.
35 G. Ballmann, S. Grams, H. Elsen and S. Harder, *Organometallics*, 2019, **38**, 2824–2833.
36 E. R. King, E. T. Hennessy and T. A. Betley, *J. Am. Chem. Soc.*, 2011, **133**, 4917–4923.
37 K. M. Carsch, A. Iliescu, R. D. McGillicuddy, J. A. Mason and T. A. Betley, *J. Am. Chem. Soc.*, 2021, **143**, 18346–18352.
38 J. Kobayashi, T. Kushida and T. Kawashima, *J. Am. Chem. Soc.*, 2009, **131**, 10836–10837.
39 A. F. Alahmadi, R. A. Lalancette and F. Jäkle, *Macromol. Rapid Commun.*, 2018, **39**, 1800456.
40 F. Vidal and F. Jäkle, *Angew. Chem., Int. Ed.*, 2019, **58**, 5846–5870.
41 Y. Ren and F. Jäkle, *Main Gr. Strateg. Towar. Funct. Hybrid Mater*, John Wiley & Sons, Ltd, Chichester, UK, 2018, pp. 79–110.
42 V. A. Wright and D. P. Gates, *Angew. Chem., Int. Ed.*, 2002, **41**, 2389–2392.
43 R. C. Smith and J. D. Protasiewicz, *J. Am. Chem. Soc.*, 2004, **126**, 2268–2269.
44 I. A. Kieffer, R. J. Allen, J. L. Fernandez, J. L. Deobald, B. L. Thompson, J. D. Wimpenny and Z. M. Heiden, *Angew. Chem., Int. Ed.*, 2018, **57**, 3377–3380.
45 Y. Dai, M. Bao, W. Wang, Z. Xie, C. Liu and Y. Su, *Chin. J. Chem.*, 2022, **40**, 2387–2392.
46 X. Wang, Z. Xie, Y. Dai, X. Liu, M. Bao, C. Liu, Q. Han, C. Liu and Y. Su, *Org. Chem. Front.*, 2023, **3**, 2949–2954.
47 A. Korzun, S. Crespi, C. Golz and A. Bismuto, *Chem. Sci. J.*, 2023, **14**, 6579–6584.
48 R. D. Rieth, N. P. Mankad, E. Calimano and J. P. Sadighi, *Org. Lett.*, 2004, **6**, 3981–3983.
49 N. Ji, H. O'Dowd, B. M. Rosen and A. G. Myers, *J. Am. Chem. Soc.*, 2006, **128**, 14825–14827.
50 V. V. Shatunov, A. A. Korlyukov, A. V. Lebedev, V. D. Sheludyakov, B. I. Kozyrkin and V. Y. Orlov, *J. Organomet. Chem.*, 2011, **696**, 2238–2251.
51 F. L. Portwich, Y. Carstensen, A. Dasgupta, S. Kupfer, R. Wyrwa, H. Görls, C. Eggeling, B. Dietzek, S. Gräfe, M. Wächtler and R. Kretschmer, *Angew. Chem., Int. Ed.*, 2022, **61**, DOI: **10.1002/anie.202117499**.
52 L. Gai, H. Lu, B. Zou, G. Lai, Z. Shen and Z. Li, *RSC Adv.*, 2012, **2**, 8840.
53 C. Duan, Y. Zhou, G.-G. Shan, Y. Chen, W. Zhao, D. Yuan, L. Zeng, X. Huang and G. Niu, *J. Mater. Chem. C*, 2019, **7**, 3471–3478.
54 J. C. Koziar and D. O. Cowan, *Acc. Chem. Res.*, 1978, **11**, 334–341.
55 Y. P. Rey, D. G. Abradelo, N. Santschi, C. A. Strassert and R. Gilmour, *Eur. J. Org. Chem.*, 2017, 2170–2178.
56 S.-M. Hyun, K. A. Reid, S. W. Vali, P. A. Lindahl and D. C. Powers, *Inorg. Chem.*, 2021, **60**, 15617–15626.
57 N. Ji, H. O'Dowd, B. M. Rosen and A. G. Myers, *J. Am. Chem. Soc.*, 2006, **128**, 14825–14827.
58 G. Q. Tian, Z. H. Yang, W. Zhang, S. C. Chen, L. Chen, G. Wu and Y. Z. Wang, *Green Chem.*, 2022, **24**, 4490–4497.
59 J. Valenta, *AIP Adv.*, 2018, **8**, 105123.
60 A. M. Brouwer, *Pure Appl. Chem.*, 2011, **83**, 2213–2228.

61 F. Neese, *Wiley Interdiscip. Rev.: Comput. Mol. Sci.*, 2022, **12**, e1606.
62 F. Neese, *Wiley Interdiscip. Rev.: Comput. Mol. Sci.*, 2018, **8**, e1327.
63 F. Neese, *Wiley Interdiscip. Rev.: Comput. Mol. Sci.*, 2012, **2**, 73–78.
64 F. Neese, F. Wennmohs, U. Becker and C. Riplinger, *J. Chem. Phys.*, 2020, **152**, 224108.
65 S. Grimme, A. Hansen, S. Ehlert and J.-M. Mewes, *J. Chem. Phys.*, 2021, **154**, 64103.
66 L. Goerigk and S. Grimme, *J. Chem. Phys.*, 2010, **132**, 184105.
67 F. Weigend and R. Ahlrichs, *Phys. Chem. Chem. Phys.*, 2005, **7**, 3297–3305.
68 M. Cossi, V. Barone, R. Cammi and J. Tomasi, *Chem. Phys. Lett.*, 1996, **255**, 327–335.